

## 2.5. TWO-DIMENSIONAL POWDER DIFFRACTION

2.5.3.3.1. *Nonuniform response correction*

A 2D detector can be considered as an array of point detectors. Each pixel may have its own response, and thus a 2D detector may exhibit some nonuniformity in intensity measurement when exposed to an isotropic source. The nonuniform response can be caused by manufacturing defects, inadequate design or limitations of the detector technology. For instance, a nonuniform phosphor screen or coupling fibre optic for a CCD detector may cause nonuniformity in quantum efficiency (Tate *et al.*, 1995). A gas-filled detector may have a different intensity response between the detector edge and centre due to the variation in the electric field from the centre to the edge. A thorough correction to the nonuniformity of the intensity response can be performed if the detector counting curves of all pixels are given. In practice, this is extremely difficult or impossible, because the behaviour of a pixel may be affected by the condition of the adjacent pixels and the whole detector. The practical way to correct the nonuniformity of the intensity response is to collect an X-ray image from an isotropic point source at the instrument centre and use the image data frame to generate a correction table for the future diffraction frames. The frame collected with the isotropic source is commonly referred to as a ‘flood-field’ frame or a flat-field image, and the correction is also called a flood-field correction or flat-field correction (Stanton *et al.*, 1992). Another type of correction for a nonuniform response is background correction. Background correction is done by subtracting a background frame from the data frame. The background frame is collected without X-ray exposure. Integrating detectors, such as image plates or CCDs, have a strong background which must be considered in nonuniform response correction. Photon-counting detectors, such as MWPC and microgap detectors, have negligible background, so background correction is not necessary.

The X-ray source for calibration for flood-field correction should be a uniform, spherically radiating point source. Identical brightness should be observed at any pixel on the detector. The radiation strength of the source should match the intensity of the diffraction data to be collected. The photon energy of the source should be the same as or close to the X-ray beam used for diffraction-data collection so that the detector behaves the same way during calibration and data collection.

There are many choices of calibration sources, including X-ray tubes, radioactive sources, diffuse scattering or X-ray fluorescence. The radioactive source Fe-55 ( $^{55}\text{Fe}$ ) is the most commonly used calibration source for a diffraction system because of its major photon energy level of 5.9 keV. X-ray fluorescence is an alternative to a radioactive source. Fluorescence emission is generated by placing a fluorescent material into the X-ray beam. Fluorescence radiation is an isotropic point source if the irradiated area is a small point-like area. For example, Cu  $K\alpha$  can produce intense fluorescence from materials containing significant amounts of iron or cobalt and Mo  $K\alpha$  can produce intense fluorescence from materials containing yttrium. In order to avoid a high localized intensity contribution from X-ray diffraction, the fluorescent material should be amorphous, such as a glassy iron foil. An alternative to a glassy alloy foil is amorphous lithium borate glass doped with the selected fluorescent element up to a 10% concentration (Moy *et al.*, 1996).

There are many algorithms available for flood-field correction depending on the nature of the 2D detector. The correction is based on the flood-field frame collected from the calibration source. The simplest flood-field correction is to normalize the counts of all pixels to the same level assuming that all pixels have

the same response curve. The corrected frame from an isotropic source is not flat, but maintains the  $\cos^3 \phi$  falloff effect, which will be considered in the frame integration. For gas-filled detectors, such as MWPC and microgap detectors, the pixel intensity response is not independent, but is affected by X-ray exposure to surrounding pixels and the whole detector. Flood-field correction is carried out by applying a normalization factor to each pixel in which a ‘rubber-sheet’ kind of stretching and shrinking in regions along the  $x$  and  $y$  detector axes slightly alters the size of each pixel (He, 2009). The total number of counts remains the same after the correction but is redistributed throughout the pixels so that the image from an isotropic source is uniformly distributed across the detector. The flood-field calibration must be done with the same sample-to-detector distance as for the diffraction-data collection.

2.5.3.3.2. *Spatial correction*

In an ideal flat 2D detector, not only does each pixel have the same intensity response, but also an accurate position. The pixels are aligned in the  $x$  and  $y$  directions with equal spacing. In most cases we assume that the detective area is completely filled by pixels, so the distance between two neighbouring pixels is equivalent to the pixel size. The deviation from this perfect pixel array is called spatial distortion. The extent of spatial distortion is dependent on the nature and limitation of the detector technology. A CCD detector with 1:1 demagnification may have a negligible spatial distortion, but the barrel distortion in the coupling fibre-optic taper can introduce substantial spatial distortion. An image-plate system may have spatial distortion caused by imperfections in the scanning system (Campbell *et al.*, 1995). MWPC detectors typically exhibit more severe spatial distortion due to the window curvature and imperfections in the wire anode (Derewenda & Helliwell, 1989).

The spatial distortion is measured from X-ray images collected with a uniformly radiating point source positioned at the instrument centre and a fiducial plate fastened to the front surface of the detector. The source for spatial correction should have a very accurate position, point-like shape and small size. The fiducial plate is a metal plate with accurately distributed pinholes in the  $x$  and  $y$  directions. The X-ray image collected with this setup contains sharp peaks corresponding to the pinhole pattern of the fiducial plate. Since accurate positions of the peaks are given by the fiducial plate, the spatially corrected image is a projection of the collected image to this plane. Therefore, the detector plane is defined as the contacting plane between the fiducial plate and detector front face.

Spatial correction restores the spatially distorted diffraction frame into a frame with correct pixel positions. Many algorithms have been suggested for spatial correction (Sulyanov *et al.*, 1994; Tate *et al.*, 1995; Stanton *et al.*, 1992; Campbell *et al.*, 1995). In the spatially corrected frame each pixel is generated by computing the pixel count from the corresponding pixels based on a spatial-correction look-up table. In a typical spatial-correction process, an image containing the spots from the calibration source passing through the fiducial plate is collected. The distortion of the image is revealed by the fiducial spots. Based on the known positions of the corresponding pinholes in the fiducial plate, the distortion of each fiducial spot can be determined. The spatial correction for all pixels can be calculated and stored as a look-up table. Assuming that the detector behaves the same way in the real diffraction-data collection, the look-up table generated from the fiducial image can then be applied to the real diffraction frames.

## 2. INSTRUMENTATION AND SAMPLE PREPARATION

The spatial calibration must be done at the same sample-to-detector distance as the diffraction-data collection.

### 2.5.3.3.3. Frame integration

2D frame integration is a data-reduction process which converts a two-dimensional frame into a one-dimensional intensity profile. Two forms of integration are generally of interest in the analysis of a 2D diffraction frame from polycrystalline materials:  $\gamma$  integration and  $2\theta$  integration.  $\gamma$  integration sums the counts in  $2\theta$  steps ( $\Delta 2\theta$ ) along constant  $2\theta$  conic lines and between two constant  $\gamma$  values.  $\gamma$  integration produces a data set with intensity as a function of  $2\theta$ .  $2\theta$  integration sums the counts in  $\gamma$  steps ( $\Delta\gamma$ ) along constant  $\gamma$  lines and between two constant  $2\theta$  conic lines.  $2\theta$  integration produces a data set with intensity as a function of  $\gamma$ .  $\gamma$  integration may also be carried out with the integration range in the vertical direction as a constant number of pixels. This type of  $\gamma$  integration may also be referred to as slice integration. A diffraction profile analogous to the conventional diffraction result can be obtained by either  $\gamma$  integration or slice integration over a selected  $2\theta$  range. Phase ID can then be done with conventional search/match methods.  $2\theta$  integration is of interest for evaluating the intensity variation along  $\gamma$  angles, such as for texture analysis, and is discussed in more depth in Chapter 5.3.

The  $\gamma$  integration can be expressed as

$$I(2\theta) = \int_{\gamma_1}^{\gamma_2} J(2\theta, \gamma) d\gamma, \quad 2\theta_1 \leq 2\theta \leq 2\theta_2, \quad (2.5.23)$$

where  $J(2\theta, \gamma)$  represents the two-dimensional intensity distribution in the 2D frame and  $I(2\theta)$  is the integration result as a function of intensity *versus*  $2\theta$ .  $\gamma_1$  and  $\gamma_2$  are the lower limit and upper limit of integration, respectively, which are constants for  $\gamma$  integration. Fig. 2.5.13 shows a 2D diffraction frame collected from corundum ( $\alpha$ -Al<sub>2</sub>O<sub>3</sub>) powder. The  $2\theta$  range is from 20 to 60° and the  $2\theta$  integration step size is 0.05°. The  $\gamma$ -integration range is from 60 to 120°. In order to reduce or eliminate the dependence of the integrated intensity on the integration interval, the integrated value at each  $2\theta$  step is normalized by the number of pixels, the arc length or the solid angle.  $\gamma$  integration with normalization by the solid angle can be expressed as

$$I(2\theta) = \frac{\int_{\gamma_1}^{\gamma_2} J(2\theta, \gamma) (\Delta 2\theta) d\gamma}{\int_{\gamma_1}^{\gamma_2} (\Delta 2\theta) d\gamma}, \quad 2\theta_1 \leq 2\theta \leq 2\theta_2. \quad (2.5.24)$$

Since the  $\Delta 2\theta$  step is a constant, the above equation becomes

$$I(2\theta) = \frac{\int_{\gamma_1}^{\gamma_2} J(2\theta, \gamma) d\gamma}{\gamma_2 - \gamma_1}, \quad 2\theta_1 \leq 2\theta \leq 2\theta_2. \quad (2.5.25)$$

There are many integration software packages and algorithms available for reducing 2D frames into 1D diffraction patterns for polycrystalline materials (Cervellino *et al.*, 2006; Rodriguez-Navarro, 2006; Boesecke, 2007). With the availability of tremendous computer power today, a relatively new method is the bin method, which treats pixels as having a continuous distribution in the detector. It demands more computer power than older methods, but delivers much more accurate and smoother results even with  $\Delta 2\theta$  integration steps significantly smaller than the pixel size. Depending on the relative size of  $\Delta 2\theta$  to the pixel size, each contributing pixel is divided into several  $2\theta$  'bins'. The intensity counts of all pixels within the  $\Delta 2\theta$  step are summarized. All the normalization methods in the above integration, either by pixel, arc or solid angle, result in an intensity

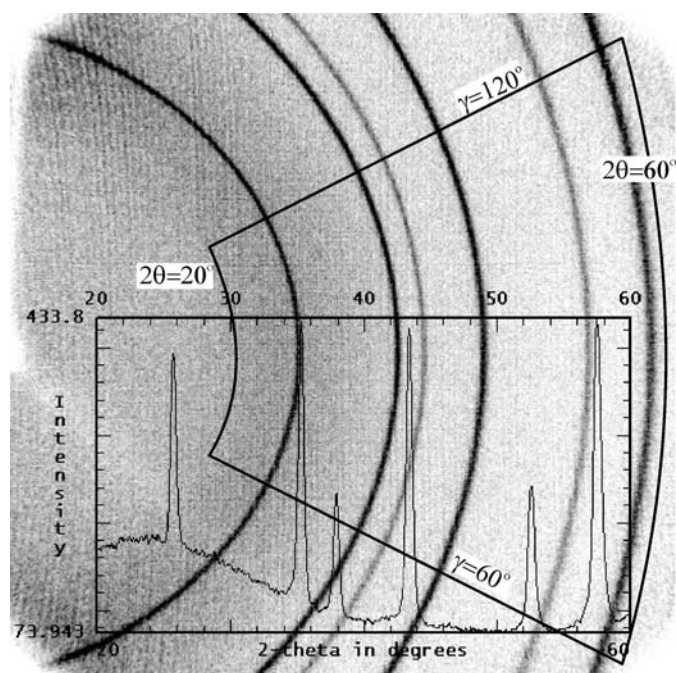


**Figure 2.5.13**

A 2D frame showing  $\gamma$  integration.

level of one pixel or unit solid angle. Since a pixel is much smaller than the active area of a typical point detector, the normalized integration tends to result in a diffraction pattern with fictitiously low intensity counts, even though the true counts in the corresponding  $\Delta 2\theta$  range are significantly higher. In order to avoid this misleading outcome, it is reasonable to introduce a scaling factor. However, there is no accurate formula for making the integrated profile from a 2D frame comparable to that from a conventional point-detector scan. The best practice is to be aware of the differences and to try not to make direct comparisons purely based on misleading intensity levels. Generally speaking, for the same exposure time, the total counting statistics from a 2D detector are significantly better than from a 0D or 1D detector.

### 2.5.3.3.4. Lorentz, polarization and absorption corrections

Lorentz and polarization corrections may be applied to the diffraction frame to remove their effect on the relative intensities of Bragg peaks and background. The  $2\theta$  angular dependence of the relative intensity is commonly given as a Lorentz-polarization factor, which is a combination of Lorentz and polarization factors. In 2D diffraction, the polarization factor is a function of both  $2\theta$  and  $\gamma$ , therefore it should be treated in the 2D frames, while the Lorentz factor is a function of  $2\theta$  only. The Lorentz correction can be done either on the 2D frames or on the integrated profile. In order to obtain relative intensities equivalent to a conventional diffractometer with a point detector, reverse Lorentz and polarization corrections may be applied to the frame or integrated profile.

The Lorentz factor is the same as for a conventional diffractometer. For a sample with a completely random orientation distribution of crystallites, the Lorentz factor is given as

$$L = \frac{\cos \theta}{\sin^2 2\theta} = \frac{1}{4 \sin^2 \theta \cos \theta}. \quad (2.5.26)$$

The Lorentz factor may be given by a different equation for a different diffraction geometry (Klug & Alexander, 1974). The forward and reverse Lorentz corrections are exactly reciprocal